

Improving the performance of Concentrating Solar Power (CSP) system using Ti/AlN/SiO₂ thin film as an alternative renewable energy source

^{*1}Bello, M., ²Sani, I. M., ³Muhammad, S.

¹Department of Physics, Federal College of Education, P.M.B 2042 Yola. Adamawa State, Nigeria

²Department of Physics, Federal College of Education, Kano, P.M.B 3045, Kano State Nigeria

³Department of Physics, Federal University of Lafia, P.M.B 146, Nasarawa State, Nigeria

*Corresponding author's email: mutawallibello2018@gmail.com Phone: +2348036041913

ABSTRACT

Successful utilization of bigger solar power systems especially concentrating solar power (CSP) as an alternative renewable energy requires not only spectrally selective absorber coatings but also, striking a balance between solar absorptance and emittance at the solar (300 nm-2500 nm) and infrared regions (>2500 nm) of solar spectrum, respectively. In the present study, we developed an ultrathin (~100 nm) tandem coating of Ti and AlN with SiO₂ as antireflection layer using magnetron sputtering system at room temperature on modified stainless steel (SS) substrate. The coating was characterized using FESEM, AFM, XRD, UV-Vis-NIR, and FTIR. 0.95 and 0.13 were respectively achieved as solar absorptance and thermal emittance. The multilayer coating exhibited good thermally stability after annealing at 500 °C in air for 2 hours. Though, optical properties of the coatings after annealing at 600 °C, was found to degrade followed by decline in absorptance and emittance from 0.95 to 0.92 and 0.13 to 0.24 respectively. These changes are associated with the decline in roughness of the coating as probed from AFM analysis. The present results show potential application of this coating in high temperature CSP system.

Keywords:

Sputtering,
Modified stainless steel
substrate,
Solar absorptance,
Thermal emittance.

INTRODUCTION

The increasing demands for electricity has led to the emergence of concentrated solar power (CSP) systems as an alternative source of energy (Bello & Shanmugan, 2022). The efficiency of CSP is influenced by the coating materials in the collector. For solar photothermal application, selective absorber coatings are required to have high solar absorptance within the wavelength range of 300 nm-2500 nm and low emittance in the infrared (IR) region at a wavelength greater than 2500 nm is required Song et al. (2017). In order to achieve the above stated desired characteristics, several approaches were made by different authors using different material combination, attacking arrangement, various deposition method, synthesis routes etc. Recently, so many tandem coatings have been studied by different researchers such as Chang et al. (2020), Rojas et al. (2021), Guo et al. (2021), Niranjana et al. (2019), AL-Rjoub et al. (2019), Wang et al. (2019), Chaoying et al. ((2021) and Wen et al. (2019). Yu et al., reported 0.936 and 0.126 as solar absorptance and thermal emittance respectively for SS/NbMaTaWN(HMVF)/NbMaTaWN(LMVF)/Al₂O₃ after annealing at 500 °C Dong-Mei et al. (2021). Ranjith et al. (2021) reported 0.981 and 0.15 as solar absorptance

and thermal emittance respectively for TiB₂/Ti (B, N)/SiON/SiO₂ and Ti/TiB₂/Ti(B, N)/SiON/SiO₂ deposited on SS substrate. Meng et al. (2018) also reported high solar absorptance and low thermal emittance of 0.953 and 0.079 at 400 °C for Cu/Zr_{0.3}Al_{0.7}N/Zr_{0.2}Al_{0.8}N/Al₃₄O₆₀N₆ MSSAC deposited on Si(111) substrate. Recently, our group developed and reported different configurations of Ti and AlN and achieved a remarkable results at high operating temperature (Bello & Shanmugan, 2022; Bello & Shanmugan, 2022 and Bello & Shanmugan, 2022). In the last decade, TiAlN coatings received great attentions owing to their outstanding stuffs like high hardness (~30-35 GPa), high oxidation resistance (~750-800 °C) and higher corrosion resistance Miao et al. (2011). Despite good performance reported in the literature, the stacking configuration is very complicated and will lead to high thickness. Also, attaining stoichiometry is a herculean task. Moreover, solar selective absorber coatings are thickness sensitive. This is because high thickness could lead to low absorption of incident solar radiation with consequence high emittance leading to low performance. In severe case, high thickness could lead to delamination

of the coating from the substrate or between coated layers in the case of multilayer coatings.

In this contribution, we report a simple and ultrathin bilayered coating comprising of Ti and AlN deposited on modified SS substrate with an antireflection (AR) layer of SiO₂ on top using sputtering deposition method at room temperature. Structural, morphological, topological and optical properties after annealing at higher temperatures were thoroughly investigated.

MATERIALS AND METHODS

Experimental procedure

Ti/AlN/SiO₂ MSSAC was prepared on modified SS substrate via DC/RF magnetron sputtering system. High purity (99.99%) Ti metal target, and dielectrics AlN and SiO₂ targets with purity of (99.99%) were used under Ar ambient. A constant Ar flow rate of 10 sccm was used throughout during the deposition. The Ti metal powered using 100 W DC source while the dielectric AlN and SiO₂ were powered using 200 W and 150 W RF source respectively. The deposition rates for Ti, AlN and SiO₂ were 1.4, 0.3 and 0.4 respectively.

Two different substrates such as SS and silicon (Si) substrates with orientation (111) were used in this study. The SS substrate with dimension (2.5 cm×2.5 cm) was cut from the as received sheet using high precision mechanical cutter. On the other hand, the Si substrate was cut to size (1.2 cm ×1.5 cm) using Si wafer scribing machine. The Si was used in this study for thickness measurement while the SS substrate was used for the main study. The SS substrates was cleaned successively in acetone and alcohol in an ultrasonic bath at 50 °C for 15 minutes and then rinsed with deionized water and dried with nitrogen purge. After cleaning, the surface of SS substrates was modified by simple annealing in air for 1 hour at 600 °C to produce rough Fe₃O₄ layer on the SS surface. The Si substrate was cleaned using Radio Corporation America (RCA) method (Al-Salman & Abdullah, 2013). In this method, three different solutions such as H₂O/NH₄OH/H₂O₂, HF/H₂O and H₂O/HCL/H₂O₂ with volume ratio (mL) 5:1:1, 1:5 and 6:1:1 respectively were prepared. The Si substrate was put into the first solution and was heated at a temperature between 75 °C to 80 °C for 10 minutes. After which, it was then transferred into the second and then third solution for 20 seconds and 10 seconds respectively while maintaining the same temperature. Finally, the Si substrate was rinsed with deionized (DI) water. After cleaning, the substrates were attached on the substrate holder and loaded into the sputtering chamber. The substrate holder was rotating continuously during the deposition process to ensure uniform coating. The vacuum chamber was pumped down to a base pressure of 5.0x10⁻⁵ mbar with the aid of a turbo pump. The shutter was closed and the targets were sputtered *in situ* for 15 minutes using Ar ion bombardments to remove impurities that might have

been embedded on it. The shutter was opened, and the deposition was carried out at room temperature. The deposition rates and the thickness were recorded from the digital crystal (thickness) monitor on the machine. The samples were subjected to thermal annealing after deposition using furnace (GSL1100X, MTI Corp.) to investigate their thermal robustness in air. The annealing was carried out by rising the temperature at the rate of 2 °C/min to the targeted temperature and allowing for 2 hours annealing at that temperature. After which, the samples were allowed to cool back to the ambient temperature.

Structural properties and chemical composition of the prepared samples were analysed with the aid of X-Ray diffractometer (XRD) and Energy-dispersive X-ray (EDX) respectively. Morphology and topology of the prepared film was studied using, Field Emission Scanning Electron Microscope (FESEM) (Model: FEI Nova NanoSEM 450) and Atomic Force Microscopy (AFM) (Model: Dimension EDGE, BRUKER). Hemispherical spectral properties of the coatings over 300 nm-2500 nm wavelength range were measured using Carry 500 UV-Vis-NIR spectrophotometer. The thermal emittance of the MSSAC was calculated from the infrared reflectance data measured over the wavelength range 5000 to 25000 nm using Furrier Transform Infrared Spectroscopy (FTIR).

The solar absorptance (α) and thermal emittance (ε) were calculated using Equations (1) and (2) respectively given by Song et al. (2017) from the measured experimental reflectance data depicted in Fig. 6a and b.

$$\alpha = \frac{\int_{\lambda_1}^{\lambda_2} (1-R(\lambda)) I_s(\lambda) d\lambda}{\int_{\lambda_1}^{\lambda_2} I_s(\lambda) d\lambda} \quad (1)$$

$$\varepsilon = \frac{\int_{\lambda_3}^{\lambda_4} (1-R(\lambda)) I_b(\lambda, T) d\lambda}{\int_{\lambda_3}^{\lambda_4} I_b(\lambda, T) d\lambda} \quad (2)$$

λ is the wavelength, λ_1 - λ_2 and λ_3 - λ_4 are the limits of integration, R is the measured experimental reflectance data and $I_s(\lambda)$ is the solar irradiance.

RESULTS AND DISCUSSION

Crystal Structure

Figure 1 depicts the XRD peaks of as-deposited alongside annealed Ti/AlN/SiO₂ MSSACs at various temperatures. The longest peak situated at an angular position $2\theta=74.76^\circ$ is related to reflection from the SS substrate. Other peaks at an angular position such as $2\theta=27.30^\circ$, 35.42° , 43.51° , and 50.74° were also recognized to be related to (400), (222), (400), (223) reflections from Fe₃O₄. Similarly, the two small peaks located at 37.90° and 59.32° are assigned to (101) and (110) reflections from AlN. The tiny peaks at 64.91° and 82.18° were also noted and are identified as (220) and (222) reflections of Ti. Bello et al., 2020 reported similar XRD patter for Ti and AlN stacked layers. There was no peak identified to be related to crystalline Ti in the as-

deposited state shown in Figure 1(a), and thus, signifying poor crystallization prior to annealing. However, an improvement in the intensity of (222) peak was noted after annealing at 400 °C and 500 °C as evidenced from Figure 1 (b) and (c) respectively, and thus indicating crystalline quality improvement with rise in temperature. It can be observed that beyond 500 °C annealing temperature, the (222) oriented peak diminishes, as

shown in Figure 1 (d) thus indicating that the crystallinity was affected by lattice defect. No any diffraction peak in all the sample identified as crystalline SiO_2 . Moreover, Chen et al. (2009) been reported that Fe_3O_4 core shell coated silica is amorphous. But the EDX spectra and the electron image (inset) shown in Figure 2 confirms the existence of silicon dioxide in the coating structure.

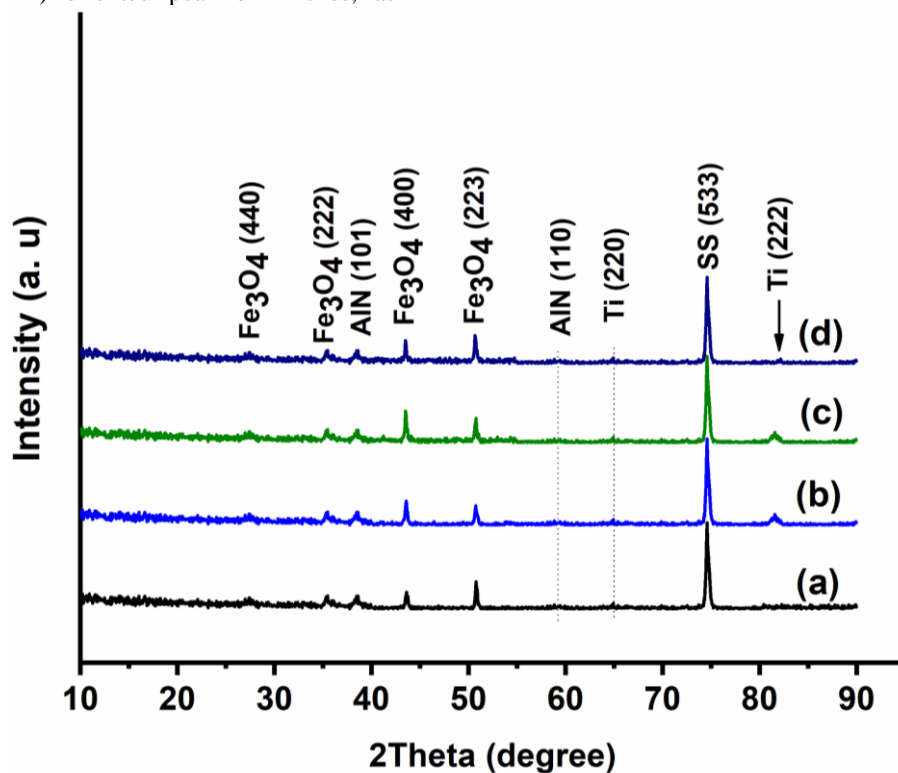


Figure 1: X-ray diffraction pattern of Ti/AlN/SiO₂ MSSAC deposited on modified SS substrate: (a) As-deposited and annealed at (b) 400 °C, (c) 500 °C and (d) 600 °C in air for 2 hours.

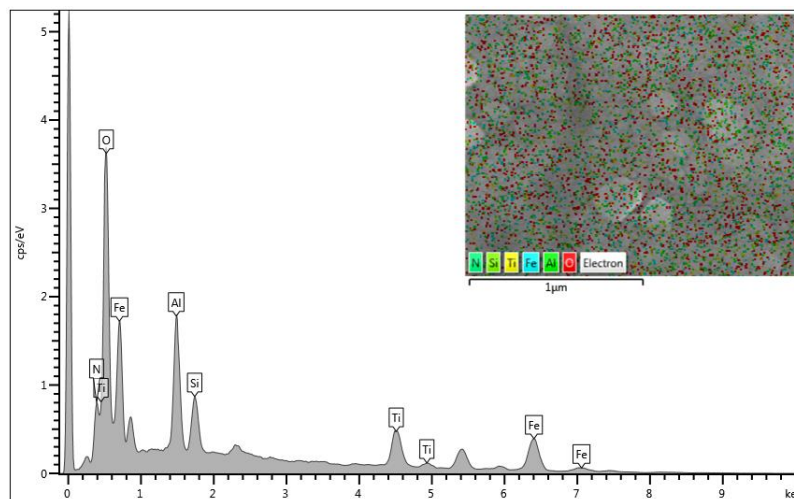


Figure 2: EDX spectra of Ti/AlN/SiO₂ MSSAC deposited on modified SS substrate.

Morphology

Figure 3(a)-(d) shows the scanning electron micrograph of as-deposited and annealed Ti/AlN/SiO₂ MSSAC for 2 hours in air. The as-deposited sample exhibited 'flake-like' nanostructures. The average size was found to be 45 ± 0.53 nm as revealed from the ImageJ analysis. The size of the flakes was found to increase with annealing temperature (Figure 3(b)-(d)) with average values

53 ± 0.47 , 61 ± 0.18 and 82 ± 0.64 nm respectively. However, an agglomeration of the nanoparticles was observed at 600 °C as shown in Figure 3(d). There was no any void or crack observed on the sample's surface despite the increase in the size of the particles, thus signifying a well compacted and adhered layers of the coating. The thickness of the individual layers is shown in Figure 4.

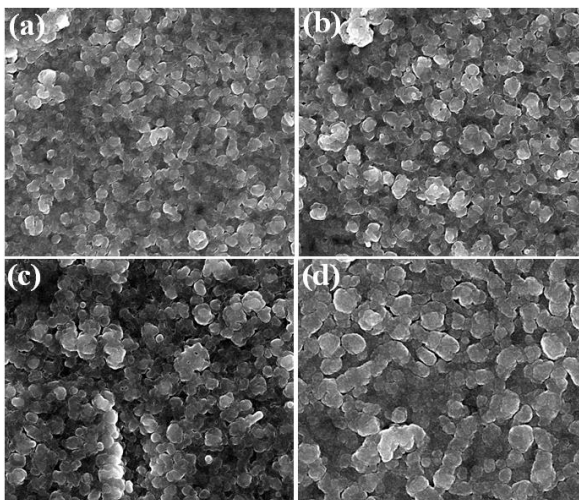


Figure 3: SEM micrographs of Ti/AlN/SiO₂ MSSAC deposited on modified SS substrate: (a) As-deposited and annealed at (b) 400 °C, (c) 500 °C and (d) 600 °C in air for 2 hours.

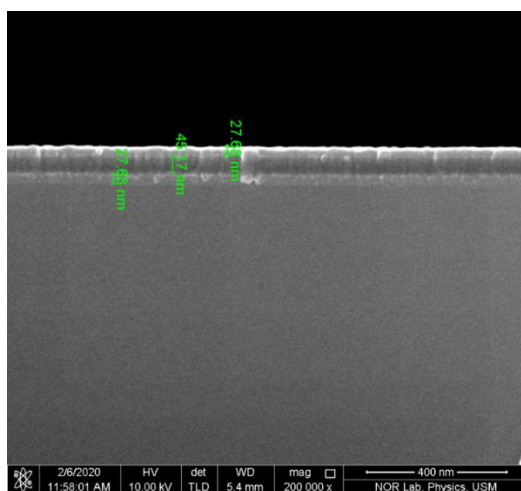


Figure 4: Cross-sectional area of Ti/AlN/SiO₂ coating

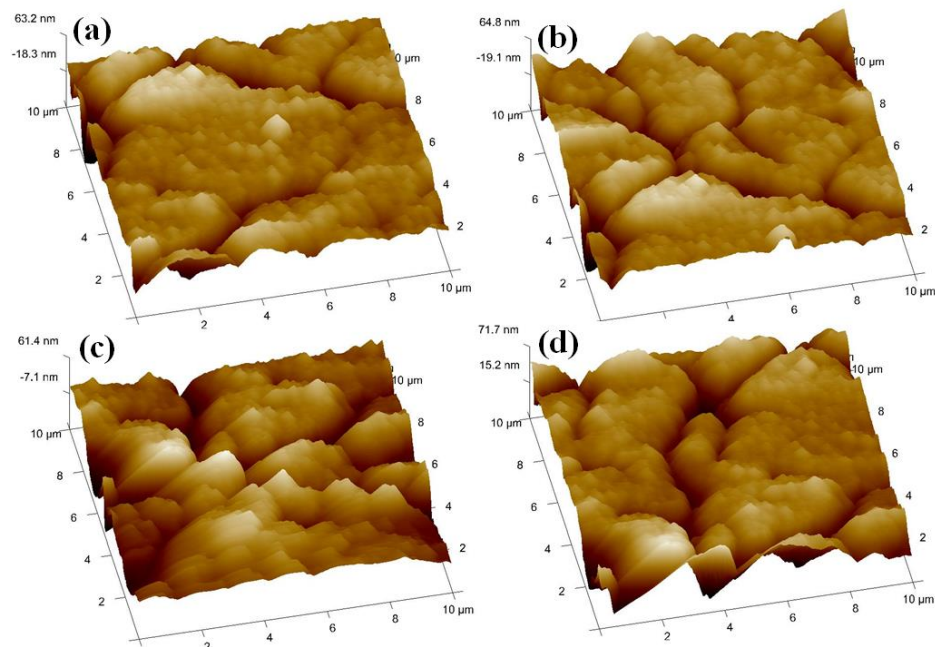


Figure 5: 3-D AFM images of Ti/AlN/SiO₂ MSSAC deposited on modified SS substrate and annealed at various temperatures in air for 2 hours.

Figure 5(a)-(d) shows the AFM images of Ti/AlN/SiO₂ MSSAC in the as-deposited state and annealed for 2 hours in air. The as-deposited sample shown in Fig 5(a) exhibits a small growth with columnar-like structures on the substrate having 34.8 nm mean roughness. After annealing at 400 °C and 500 °C, the mean surface roughness has increased from 34.8 nm to 48.7 nm and 53.5 nm respectively. However, at 600 °C a decline in the surface roughness value from 53.5 nm to 51.2 nm was noted. This could be due to the decrease in the crystalline quality of the film as observed in the XRD analysis. These topological features of the coating are consistent with the spectral properties of the post annealed samples. According to (Farooq & Lee, 2003), surface roughness is important as it reduces reflections from the surface of the sample, thereby enhancing solar absorption as a result of multiple reflections of reflected light. Moreover, Feng et al. (2015) reported that, roughness between 10 nm -100 nm can support absorption of solar radiation with slightly raise in emittance value, leading to a good solar selectivity. Fortunately, the surface roughness of the present MSSAC is within the range stated above, which is responsible for the high solar absorption.

Spectral properties Ti/AlN/SiO₂ MSSAC

The hemispherical reflectance spectra of bare and modified SS substrate, as-deposited and the heat treated Ti/AlN/SiO₂ MSSAC at various temperatures in air for 2 hours within the solar range of 300 nm-2500 nm along side that of the IR region within the range of 5000 nm-25000 nm is shown in Fig. 6(a) and (b). Reflectance of

bare and modified SS substrates were used for reference purpose. From Fig. 6a, it can be observed that the bare SS substrate exhibits high reflectance especially beyond 800 nm and it increases towards longer wavelength. This behaviour exhibited by the SS substrate is required for high temperature photothermal conversion applications. It can be observed that after modification of the SS substrate, the reflectance of the bare was suppressed especially within 300 nm-1830 nm. A small interference curve was observed within 330 nm-460 nm for the modified substrate. This could be associated with the light interference within the visible region of solar spectrum. After depositing the whole tandem coating of Ti/AlN/SiO₂, there was a huge decrease in the reflectance throughout the entire wavelength range of 300 nm- 2500 nm, and thus, indicating high solar absorptance. To study the stability of the present coating in air at high temperature, three samples were annealed at 400 °C, 500 °C and 600 °C. The reflectance spectra of the post annealed samples are depicted in Fig. 6a. There was no significance difference in the reflectance spectra after annealing up to 500 °C, and hence indicating good stability of the present coating at higher temperatures. In all the samples, between 500 nm-1000 nm, a broad peak in reflectance spectra was observed. These peaks are due to the interactions of incident and reflected light and also electronic transition within the coated layers of the coatings Wattoo et al. (2016). The thermal emittance of the coating was calculated from the IR reflectance spectra depicted in Fig. 6b. The reflectance from bare substrate has increased after modification, and hence indicating

drop in the emittance value. The reflectance increased further after deposition of Ti/AlN/SiO₂ MSSAC. After annealing at 400 °C and 500 °C, there was improvement in IR reflectance. Beyond 500 °C annealing temperature,

however, a decline in the reflectance spectra was observed (see dotted lines for sample annealed at 600 °C) and hence indicating rise in the emittance value.

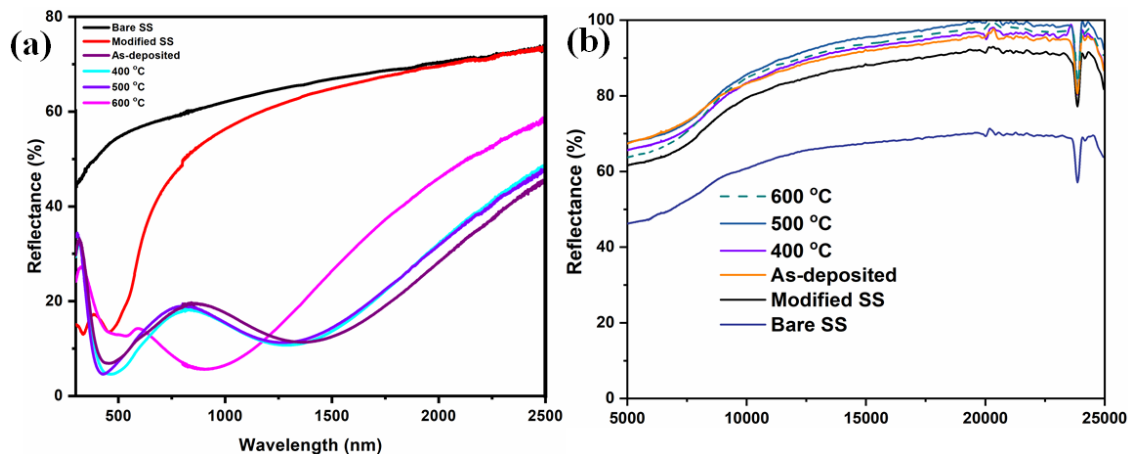


Figure 6: Reflectance spectra of reference pristine SS substrate, modified SS substrate and the whole Ti/AlN/SiO₂ MSSAC deposited on modified SS substrate and annealed at different temperatures in air for 2 hours.

The bare and modified SS substrate exhibits 0.35 and 0.43 solar absorptance and 0.25 and 0.10 thermal emittance respectively. The improvement in the absorptance value after modification is due to rough Fe₃O₄ formation which is responsible for trapping of reflected light. After depositing the whole tandem coating of Ti/AlN/SiO₂ prior to annealing, an improved value of solar absorptance of 0.93 was achieved with emittance of 0.12. The rise in the emittance value after deposition of the coating is due to the thickness. Usually thicker coatings are known to enhance emittance. After annealing at 400 °C and 500 °C, an improvement in the solar absorptance from 0.93 to 0.94 and 0.95 with rise in thermal emittance from 0.12 to 0.13 and 0.15 was recorded. The increase in the solar absorptance value is associated with the improvement in the crystal quality of the film as probed from the XRD analysis. A huge decline in the solar absorptance value from 0.95 to 0.92 with rise in emittance from 0.15 to 0.24 after annealing at 600 °C was observed, thus indicating deterioration in the optical properties of the coating. This results are in good agreement with the XRD analysis presented in Fig. 1.

CONCLUSION

Ti/AlN/SiO₂ coatings were prepared via DC/RF magnetron sputtering on modified SS substrate at room temperature. The coatings demonstrated high thermal stability even after annealing at 500 °C with registered 0.95 and 0.13 as solar absorptance and thermal emittance. However, upon annealing at 600 °C, a decrease in the solar absorptance from 0.95 to 0.92 followed by rise in the emittance value from 0.13 to 0.24 was noticed, hence

indicating degradation of the optical properties of the present coating as evidenced from the XRD analysis for the sample annealed at 600 °C where the intensity of (222) oriented peak was found to be diminishing. The absence of void or crack on the coating's surface signifies good adhesion between the coated layers and the substrate. These results suggest the potentials application of Ti/AlN/SiO₂ coatings in high temperature CSP system.

ACKNOWLEDGEMENT

The authors would like to acknowledge Universiti Sains Malaysia (USM), Nano Optoelectronic Research Laboratory (NORL) and Thermal Management Research Laboratory USM for using their Lab facilities in carrying out this research.

REFERENCES

- Al-rjoub, A., Rebouta, L., Costa, P., Cunha, N. F., Lanceros-mendez, S., Barradas, N. P., Alves, E. (2019). Applied Surface Science The effect of increasing Si content in the absorber layers (CrAlSiN_x/CrAlSiO_yN_x) of solar selective absorbers upon their selectivity and thermal stability. *Applied Surface Science Journal*, 481 1096–1102. <https://doi.org/10.1016/j.apsusc.2019.03.208>
- Al-Salman, H. S., Abdullah, M. J. (2013). RF sputtering enhanced the morphology and photoluminescence of multi-oriented ZnO nanostructure produced by chemical vapor deposition. *J. Alloys Compd.*, 547 132–137
- Bello, M., Shanmugan, S. (2022). Investigation of in-plane heat distribution, thermal stability and mechanical

properties of SS-(Fe₃O₄)/Ti/AlN/Ti/SiO₂ as absorber coatings for efficient high temperature concentrated solar power systems. *Journal of Alloys and Compounds*, 901 163576. <https://doi.org/10.1016/j.jallcom.2021.163576>

Bello, M., Shanmugan, S. (2022). *High-temperature AlN and Ti multilayer cermet for solar absorber coating: structural and optical properties. Indian Journal of Physics*. <https://doi.org/10.1007/s12648-022-02334-y>

Bello, M., Subramani, S. (2022). *Growth, characterisation and thermal stability of AlN/Ti/AlN/SiO₂ multilayer selective solar absorber coating for high temperature applications. International Journal of Nanotechnology*. 19 (2/3/4/5) 252–264.

Bello, M., Subramani, S., Marzaini, M. M, B. (2020). The impact of Fe₃O₄ on the performance of ultrathin Ti/AlN/Ti tandem coating on stainless-steel for solar selective absorber application. *Results in Physics*, 103582. <https://doi.org/10.1016/j.rinp.2020.103582>

Chang, Y., Yang, Y., Weng, S. (2020). Surface & Coatings Technology Effect of interlayer design on the mechanical properties of AlTiCrN and multilayered AlTiCrN/TiSiN hard coatings. *Surface & Coatings Technology*, 389.

Chaoying, L., Zhiqiang, S., Feng, H., Hebin, Z., Juanrong, M. (2021). Design, synthesis and thermal stability study on graded TiN_xO_y solar selective absorbing coating fabricated by pulsed DC reactive magnetron sputtering. *Materials Characterization*, 173 110921. <https://doi.org/10.1016/j.matchar.2021.110921>

Chen, J., Wang, Y. G., Li, Z. Q., Wang, C., Li, J. F., Gu, Y. J. (2009). Synthesis and characterization of magnetic nanocomposites with Fe₃O₄ core. *Journal of Physics: Conference Series*, 152. <https://doi.org/10.1088/1742-6596/152/1/012041>

Farooq, M., Lee, Z. H. (2003). Computations of the optical properties of metal/insulator-composites for solar selective absorbers. *Renewable Energy*, 28(9), 1421–1431. [https://doi.org/10.1016/S0960-1481\(02\)00033-2](https://doi.org/10.1016/S0960-1481(02)00033-2).

Feng, J., Zhang, S., Liu, X., Yu, H., Ding, H., Tian, Y., Ouyang, J. (2015). Solar selective absorbing coatings TiN/TiSiN/SiN prepared on stainless steel substrates. *Vacuum*, 121, 135–141. <https://doi.org/10.1016/j.vacuum.2015.08.013>

Guo, H. X., Yu, D. M., He, C. Y., Qiu, X. L., Zhao, S. S., Liu, G., Gao, X. H. (2021). Double-layer solar absorber coating based on high entropy ceramic AlCrMoTaTiN: Structure, optical properties and failure mechanism.

Surfaces and Interfaces, 24 101062. <https://doi.org/10.1016/j.surfin.2021.101062>.

Miao Du, Lei Hao, Xiaopeng Liu, Lijun Jiang, Shumao Wang, Fang Lv, Zhinian Li, J. M. (2011). Microstructure and thermal stability of Ti_{1-x}Al_xN coatings deposited by reactive magnetron co-sputtering. *Physics Procedia*, 18 222–226. <https://doi.org/10.1016/j.phpro.2011.06.085>.

Niranjan, K., Kondaiah, P., Srinivas, G., Barshilia, H. C. (2019). Optimization of W/WAlSiN/SiON/SiO₂ tandem absorber consisting of double layer anti-reflection coating with broadband absorption in the solar spectrum region. *Applied Surface Science*, 496 143651. <https://doi.org/10.1016/j.apsusc.2019.143651>.

Ranjith, K. P., Basavaraju, U., Barshilia, H. C., Basu, B. (2021). Solar Energy Materials and Solar Cells On the origin of spectrally selective high solar absorptance of TiB₂-based tandem absorber with double layer antireflection coatings. *Solar Energy Materials and Solar Cells*, 220.

Rojas, T. C., Caro, A., Lozano, G., S, J. C. (2021). Solar Energy Materials and Solar Cells High-temperature solar-selective coatings based on Cr(Al)N. Part 1: Microstructure and optical properties of CrN_y and Cr_{1-x}Al_xN_y films prepared by DC/HiPIMS. *Solar Energy Materials and Solar Cells Journal*, 223.

Jian-Ping, M., Rui-rui, G., Hu, L., Lu-ming, Z., Xiaopeng, L., Zhuo, L. (2009). Microstructure and thermal stability of Cu/Zr_{0.3}Al_{0.7}N/Zr_{0.2}Al_{0.8}N/Al₃₄O₆₀N₆ cermet-based solar selective absorbing coatings. *Applied Surface Science Journal*, 255, 7918–7924.

Song, P., Wu, Y., Wang, L., Sun, Y., Ning, Y., Zhang, Y., Dai, B., Tomasella, E., Bousquet, A., Wang, C. (2017). The investigation of thermal stability of Al/NbMoN/NbMoON/SiO₂ solar selective absorbing coating. *Solar Energy Materials and Solar Cells*, 171 253–257. <https://doi.org/10.1016/j.solmat.2017.06.056>

Wang, X., Luo, T., Li, Q., Cheng, X., Li, K. (2019). Solar Energy Materials and Solar Cells High performance aperiodic metal-dielectric multilayer stacks for solar energy thermal conversion. *Solar Energy Materials and Solar Cells*, 191 372–380. <https://doi.org/10.1016/j.solmat.2018.12.006>

Wattoo, A. G., Xu, C., Yang, L., Ni, C., Yu, C., Nie, X., Yan, M., Mao, S., Song, Z. (2016). Design, fabrication and thermal stability of spectrally selective TiAlN/SiO₂ tandem absorber. *Solar Energy*, 138, 1–9. <https://doi.org/10.1016/j.solener.2016.08.053>

Wen, H., Wang, W., Wang, W., Su, J., Lei, T., Wang, C. (2019). Enhanced spectral absorption of bilayer WO_x/SiO_2 solar selective absorber coatings via low vacuum pre-annealing. *Solar Energy Materials and Solar Cells*, 202(May), 110152. <https://doi.org/10.1016/j.solmat.2019.110152>

Y. Dong-Mei, Cheng-Yu He, Xiao-Li Qiu, Shuai-Sheng Zhao, Hui-Xia Guo, Gang Liu, X-H G. (2021). A multilayer solar absorber coating based on NbMoTaW refractory high entropy alloy: Optical properties, thermal stability and failure mechanism. *Materials Today Energy*. <https://doi.org/https://doi.org/10.1016/j.mtener.2021.100789>.